

A Bayesian inference approach to identify a Robin coefficient in one-dimensional parabolic problems[☆]

Liang Yan^{*}, Fenglian Yang, Chuli Fu^{*}

School of Mathematics and Statistics, Lanzhou University, Lanzhou 730000, China

ARTICLE INFO

Article history:

Received 8 December 2008

Received in revised form 28 April 2009

Keywords:

Bayesian inference approach
Robin coefficient
Inverse heat transfer problems
Markov chain Monte Carlo
Hierarchical Bayesian model

ABSTRACT

This paper investigates a nonlinear inverse problem associated with the heat conduction problem of identifying a Robin coefficient from boundary temperature measurement. A Bayesian inference approach is presented for the solution of this problem. The prior modeling is achieved via the Markov random field (MRF). The use of a hierarchical Bayesian method for automatic selection of the regularization parameter in the function estimation inverse problem is discussed. The Markov chain Monte Carlo (MCMC) algorithm is used to explore the posterior state space. Numerical results indicate that MRF provides an effective prior regularization, and the Bayesian inference approach can provide accurate estimates as well as uncertainty quantification to the solution of the inverse problem.

© 2009 Elsevier B.V. All rights reserved.

1. Introduction

Inverse heat transfer problems (IHTP) have numerous important applications in various branches of engineering and science, including the determination of the boundary condition, thermal properties, unknown heat source, and unknown heat transfer coefficients, etc. A typical feature of the IHTP compared to well-posed direct heat transfer problems is that the existence, uniqueness and stability of their solutions are not always guaranteed, see e.g. [1]. For some discussion of inverse techniques for heat transfer problems, one can consult Alifanov [2] and Beck et al. [3].

In this paper, we are interested in estimating the heat transfer coefficient, hereafter denoted as the Robin coefficient, of a parabolic problem, which models the convection between the conduction body and the ambient environment, from overspecified surface temperature. This inverse problem has recently received the attention of many mathematical studies. Studies on the uniqueness and conditional stability can be found in [4–6]. Several numerical methods have been proposed for determining the heat transfer coefficient. Masson et al. [7] have applied the iterative regularization to estimate the two-dimensional heat transfer coefficient. Yang et al. [8] applied an iterative method, namely the conjugate gradient method, to estimate the heat coefficient, while the finite difference method (FDM) was employed to discretize the parabolic equation. Ling et al. [9] have applied a noniterative finite element-based inverse method to estimate the heat transfer coefficient. The boundary element method with the overspecified data on the boundaries has been studied in [10,11]. Recently, Chen and Wu [12] proposed a hybrid inverse method to predict the distribution of the heat transfer coefficient and surface heat flux for two-dimensional heat transfer coefficient. Besides, the sequential function specification method [13,14] has also been used in estimating the transient heat transfer coefficient.

The above deterministic inverse techniques based on exact matching or least-squares optimizations, yield only a point estimate of unknowns without rigorously considering and analyzing stochastic nature of the measurement errors and without quantifying the associated uncertainty in the inverse solution. However, in practical applications, uncertainties

[☆] The project is supported by the National Natural Science Foundation of China (Nos. 10671085, 10571079) and the program of NCET.

^{*} Corresponding author.

E-mail addresses: yanl8310@yahoo.com.cn, yanliang06@lzu.cn (L. Yan), fuchuli@lzu.edu.cn (C. Fu).

are ubiquitous since the data are always contaminated by the inherent measurement errors and only known with certain confidence. Meanwhile, the forward model may be imperfect and imprecise due to the presence of unmodeled physics. Hence, it is necessary to incorporate these uncertainties in the inverse methodology. Recently, several methods for the inverse analysis under uncertainties have been proposed, e.g. sensitivity analysis [15], the extended maximum likelihood method [16], the spectral stochastic method [17,18], and the Bayesian inference approach [19].

Among the solution methods considered, the Bayesian inference method has a number of distinctive attributes. In Bayesian inference, a prior distribution model is combined with the likelihood to formulate the posterior probability density function (PPDF). From this posterior distribution, one can estimate means, modes, marginal distribution and credible intervals by averaging over the posterior. Even when seeking only a point estimate, the Bayesian method can provide more flexible regularization in the sense that the nontrivial problem of selecting an appropriate regularization parameter is resolved through hierarchical Bayesian models. With the recent propagation of Markov chain Monte Carlo (MCMC) [20] methods, the Bayesian inference approach has attracted much interest in diverse applied inverse problems, including geophysics [21], image processing [22], and heat conduction problems [23–25].

In this work, we extend the Bayesian inference method to reconstruct the Robin coefficient distribution on a boundary surface in one-dimensional transient inverse heat transfer problems. More recently, Jin [26] employed the Bayesian inference approach to recover the Robin coefficient in steady-state heat conduction problems. Parthasarathy and Balaji [27] proposed the Bayesian inference approach to estimate scalar heat transfer coefficient from boundary measurement for the unsteady-state heat conduction, but they only consider the heat transfer coefficients to be constants. Nevertheless, publications have not been found so far to use this method for solving the inverse problem of determining the Robin coefficient which is taken to be time-dependent in the parabolic equation.

The outline of the paper is as follows. Section 2 introduces the mathematical definition of the problem, and discusses its finite difference discretization. Section 3 introduces the general framework of Bayesian inference with an emphasis on hierarchical Bayesian models. The numerical exploration of the posterior state space via the MCMC is discussed in Section 4. Several numerical examples are presented in Section 5 to illustrate the efficiency of the numerical algorithm. Finally, in Section 6, some concluding remarks are given.

2. Mathematical formulation of the problem

In this section, we start by discussing the mathematical model for the problem of determining the Robin coefficient of the parabolic equation. The implementation of the forward problem with a finite difference approximation is also discussed in detail.

2.1. Mathematical model

Consider the following initial boundary value problem for the parabolic equation

$$\frac{\partial u}{\partial t}(x, t) = \frac{\partial^2 u}{\partial x^2}(x, t), \quad (x, t) \in Q := (0, 1) \times (0, t_f], \quad (2.1)$$

$$u(x, 0) = g(x), \quad x \in [0, 1], \quad (2.2)$$

$$-\frac{\partial u}{\partial x}(0, t) + \rho(t)u(0, t) = h_0(t), \quad t \in [0, t_f], \quad (2.3)$$

$$\frac{\partial u}{\partial x}(1, t) + \rho(t)u(1, t) = h_1(t), \quad t \in [0, t_f], \quad (2.4)$$

where $t_f > 0$ is an arbitrary fixed time of interest, g , h_0 , h_1 are given functions, and u represents the temperature. $\rho(t) \geq 0$ is the time-dependent heat transfer coefficient representing the corrosion damage. Classically, it is interpreted as a Robin coefficient of energy exchange and characterise the contribution that an interface makes to the overall thermal resistance to the system and is defined in terms of the heat flux across the surface for a unit temperature gradient. Notice that if $\rho(t)$ is given, the problem (2.1)–(2.4) is a well-posed direct problem, which has been extensively studied. Unfortunately, in many practical situations, the characteristics of the heat transfer coefficient are always unknown. Therefore, the problem is mathematically under-determined and additional data must be supplied to fully determine the physical process. In this paper, the overspecified condition is given by the following measurement data

$$Y(t) = u(1, t), \quad t \in [0, t_f]. \quad (2.5)$$

Let us denote with $\mathbf{F}(\rho)$ the vector of computed temperatures at the boundary $x = 1$, where the operator \mathbf{F} is defined by $\mathbf{F} : \rho \mapsto u(1, t; \rho)$. Then the inverse problem is to solve the following nonlinear operator equation

$$\mathbf{F}(\rho) = Y. \quad (2.6)$$

Like most inverse problems, the inverse Robin problem is also ill-posed [8], i.e. the existence, uniqueness and stability of its solution are not always guaranteed. In practice, the measurement data inevitably contaminated with errors that may cause large deviations of the solution from the exact one. In this work, we use Bayesian inference approach to deal with the instability of the inverse problem.

In the Bayesian statistical inverse approach, all the variables included in the model are modeled as random variables. In contrast to the traditional formulation of the inverse problem, the solution of the Bayesian statistical inverse problem is the conditional probability density function of the unknown parameters given the measurement. This conditional density function is called the posterior probability density function (PPDF) and can be derived according to Bayes' formula:

$$p(\rho|Y) \propto p(Y|\rho)p(\rho), \quad (3.1)$$

where $p(\rho|Y)$ is the PPDF, the function $p(Y|\rho)$ and $p(\rho)$ are known as the likelihood and the prior density function, respectively.

The construction of the likelihood function is often the most straightforward part in the Bayesian statistical inversion. A most common and simple model assumes that the random errors in Eq. (2.7) are independent identically distributed (i.i.d.) Gauss random noise with zero mean and standard deviation σ . Then the likelihood $p(Y|\rho)$ can be written as

$$p(Y|\rho) \propto (\sigma^2)^{-ny/2} \exp\left(-\frac{(\mathbf{F}(\rho) - Y)^T(\mathbf{F}(\rho) - Y)}{2\sigma^2}\right), \quad (3.2)$$

where ny is the dimension of the vector Y .

In the Bayesian inference approach to inverse problems, the construction of the a priori density is the most crucial step. A useful tool for prior modeling is Markov random field (MRF). The MRF model has been shown to perform well in several application areas. For a further insight, one may refer to [23,25]. In the current study, the following simple MRF is taken:

$$p(\rho) \propto \lambda^{m/2} \exp\left(-\frac{1}{2}\lambda\rho^T\mathbf{W}\rho\right), \quad (3.3)$$

where m is the dimension of the vector ρ , λ is a scaling parameter. The entries of the $m \times m$ symmetric matrix \mathbf{W} are determined as $\mathbf{W}_{ij} = n_i$ if $i = j$, $\mathbf{W}_{ij} = -1$ if i and j are adjacent, and 0 otherwise. Here, n_i is the number of neighbors adjacent to site i .

With likelihood (3.2) and the prior model (3.3), the PPDF $p(\rho|Y)$ can be evaluated as

$$p(\rho|Y) \propto \exp\left(-\frac{(\mathbf{F}(\rho) - Y)^T(\mathbf{F}(\rho) - Y)}{2\sigma^2}\right) \exp\left(-\frac{1}{2}\lambda\rho^T\mathbf{W}\rho\right). \quad (3.4)$$

From the PPDF, various point estimators can be computed such as the posterior conditional mean (CM) estimator

$$\hat{\rho}_{\text{CM}} = E(\rho|Y) \quad (3.5)$$

and the maximum *a posteriori* (MAP) estimator

$$\hat{\rho}_{\text{MAP}} = \operatorname{argmax}_{\rho} p(\rho|Y). \quad (3.6)$$

The MAP estimate of ρ can then be derived as:

$$\hat{\rho}_{\text{MAP}} = \operatorname{argmin}_{\rho} \{(\mathbf{F}(\rho) - Y)^T(\mathbf{F}(\rho) - Y) + \lambda\sigma^2\rho^T\mathbf{W}\rho\}, \quad (3.7)$$

which is exactly similar to the Tikhonov regularization method. Therefore, the prior distribution provides regularization to the inverse problem and λ assumes the role of a regularization parameter. However, the selection of the regularization parameter has never been trivial in almost all deterministic inverse techniques. The Bayesian inference approach addresses the issue flexibly by letting the data determine an appropriate regularization parameter and thus provides an elegant approach to choose λ automatically. The parameter λ in (3.3) can be treated as random variables in Bayesian inference, which is often termed as hyper-parameter. A hierarchical Bayesian PPDF is then formulated as follows:

$$p(\rho, \lambda|Y) \propto p(Y|\rho, \lambda)p(\rho|\lambda)p(\lambda). \quad (3.8)$$

A standard way to select priors for the hyper-parameters is to use the conjugate priors [29]. For Eq. (3.8), Gamma distribution is chosen as a prior for λ

$$p(\lambda) \propto \lambda^{\alpha-1} e^{-\beta\lambda}. \quad (3.9)$$

With the hyper-priors defined above, a hierarchical Bayesian posterior distribution can be computed as follows:

$$p(\rho, \lambda|Y) \propto \exp\left(-\frac{(\mathbf{F}(\rho) - Y)^T(\mathbf{F}(\rho) - Y)}{2\sigma^2}\right) \lambda^{m/2} \exp\left(-\frac{1}{2}\lambda\rho^T\mathbf{W}\rho\right) \lambda^{\alpha-1} e^{-\beta\lambda}. \quad (3.10)$$

4. Posterior state space exploration

In most of the cases, the PPDF (3.10) is nonstandard and implicit, and the dimension of the posterior state space may be high. Due to the above reasons, statistical sampling algorithms such as MCMC simulation must be introduced to explore the posterior state space. In the following of this section, ρ denotes the unknown random vector, $p(\rho)$ denotes any probability density function of ρ .

The idea of general Monte Carlo simulation is to draw a set of i.i.d. samples $\{\rho^{(i)}\}_{i=1}^L$ from the target distribution $p(\rho)$, where L is the size of the sample set. For the PPDF (3.10), the key step in Monte Carlo simulation is to draw the sample set from this high dimensional and implicit distribution function. Among various sampling strategies, the MCMC is the most powerful and popular one.

The essence of MCMC algorithms is to explore the state space of a random parameter using the Markov chain mechanism. The literature on MCMC methods is extensive. For a complete discussion of this algorithm, we refer to Ref. [20]. In this paper, the PPDF $p(\rho, \lambda|Y)$ is sampled using the following hybrid of the Metropolis–Hastings algorithm and the Gibbs algorithm:

```

1. Initialize  $\rho^{(0)}, \lambda^{(0)}$ 
2. For  $i = 0 : N_{mcmc} - 1$ 
  sample  $\rho^{(*)} \sim q(\rho|\rho^{(i)})$ 
  sample  $u \sim U(0, 1)$ 
  if  $u < A(\rho^{(*)}, \rho^{(i)})$ 
     $\rho^{(i+1)} = \rho^{(*)}$ 
  else  $\rho^{(i+1)} = \rho^{(i)}$ 
  sample  $\lambda^{(i+1)} \sim p(\lambda^{(i)}|\rho^{(i+1)})$ 

```

where $A(\rho^{(*)}, \rho^{(i)}) = \min\{1, \frac{p(\rho^{(*)}, \lambda^{(i)}|Y)q(\rho^{(i)}|\rho^{(*)})}{p(\rho^{(i)}, \lambda^{(i)}|Y)q(\rho^{(*)}|\rho^{(i)})}\}$.

In the above algorithm, N_{mcmc} is the length of the Markov chain, and $\rho^{(i)}, \lambda^{(i)}$ are the samples generated in the i th iteration for ρ, λ , respectively. u is a random number generated from the standard uniform distribution $U(0, 1)$ and $q(\rho|\rho^{(i)})$ is the easy-to-sample proposal distribution for ρ . The full conditional $p(\lambda|\rho)$ can be derived as

$$p(\lambda|\rho) \propto \lambda^{m/2+\alpha-1} \exp\left(-\frac{1}{2}(\rho^T \mathbf{W} \rho + \beta)\lambda\right).$$

Once the designed Markov chain converges, the samples recorded thereafter are from the target posterior distribution Eq. (3.10). The posterior condition mean estimates can then be computed using these samples.

5. Numerical experiments

In this section we illustrate the efficiency and accuracy of the Bayesian inference approach by several numerical examples. For simplicity, we always set $t_f = 1$ and $g(x) = x^2 + 1$, $h_0(t) = t(2t + 1)$, $h_1(t) = 2 + 2t(t + 1)$.

For the test cases examined, the problems were numerically solved by using MATLAB software. The initial guess for ρ, λ in the hybrid algorithm is taken to be 0 and 10, respectively. The length N_{mcmc} of the Markov chain is taken to be 10 000, and the last 5000 realizations are used to compute the estimates. For the results presented below, we consider $h = \tau = 0.1$ for Example 1, and $h = \tau = 0.05$ for Examples 2 and 3. Unless otherwise specified, the values of α and β chosen are $\alpha = 50$, $\beta = 0.1$ following [26]. The proposal distribution $q(\rho|\rho^{(*)})$ is a random walk sampler $q(\rho|\rho^{(*)}) \sim N(\rho^{(*)}, \sigma_\rho^2)$ with the scale parameter $\sigma_\rho = 0.04$. The synthetic noisy data are generated by

$$Y_i = (\mathbf{F}(\rho))_i + \max_{1 \leq i \leq ny} \{ |(\mathbf{F}(\rho))_i| \} \epsilon \omega, \quad i = 1, \dots, ny \quad (5.1)$$

where ϵ dictates the relative noise level and ω is a Gaussian random variable with zero mean and unit standard deviation. In our computations, ω is realized using the Matlab function *randn*.

To measure the accuracy of the numerical solution $\rho(t)$, we use the following relative error $\text{rel}(\rho)$ defined as

$$\text{rel}(\rho) = \frac{\sqrt{\sum_{i=1}^m (\rho_i - \hat{\rho}_i)^2}}{\sqrt{\sum_{i=1}^m (\rho_i)^2}} \quad (5.2)$$

where $\hat{\rho}_i$ and ρ_i are the numerical and exact solutions evaluated at a point t_i , respectively.

5.1. Smooth solution

Example 1. The Robin coefficient $\rho(t)$ is a smooth function

$$\rho(t) = t, \quad 0 \leq t \leq 1. \quad (5.3)$$

This example is a typical benchmark problem considered in Refs. [8,10,11] and it is investigated here for comparison purpose. In this example, the direct problem (2.1)–(2.4) has an analytical solution

$$u(x, t) = x^2 + 2t + 1. \quad (5.4)$$

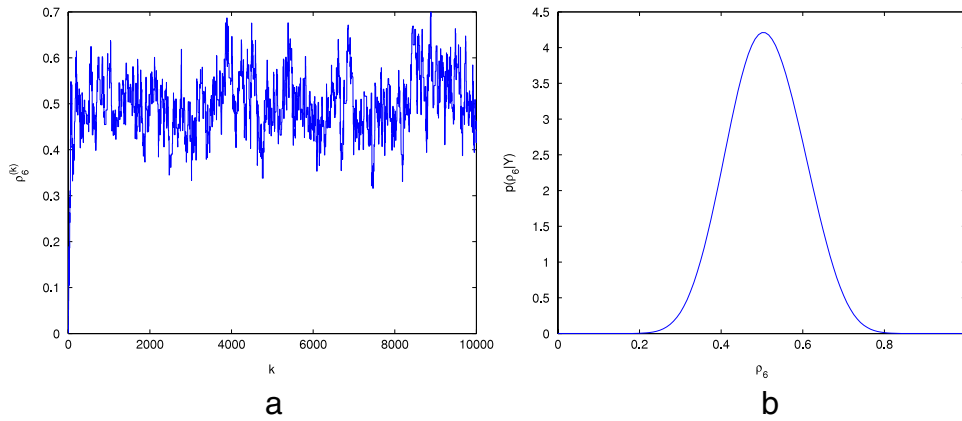


Fig. 1. (a) The trace plot of ρ_6 and (b) its posterior density for Example 1 with 5% noise added into the data.

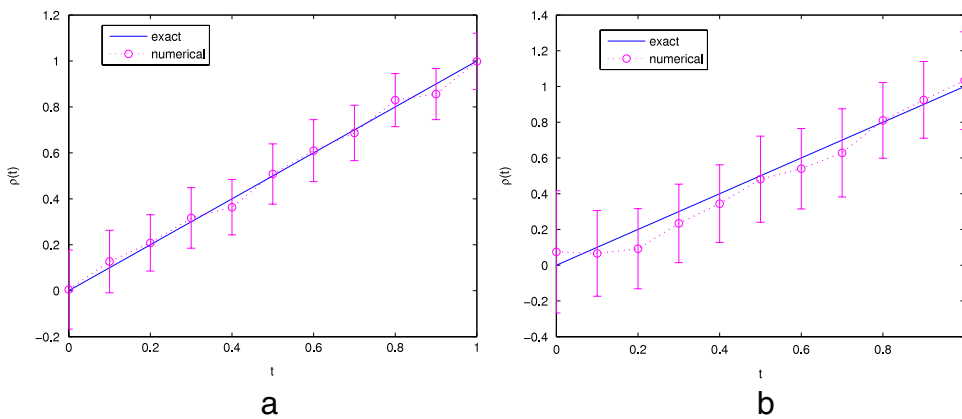


Fig. 2. The numerical results for Example 1 with (a) 1% and (b) 5% noise added into the data.

It is important to check the convergence and mixing of the chain before analyzing the result. The simplest way is by visualizing the trace plots of the chain. As a typical sample, we display the trace plot of the Markov chain for the component ρ_6 in Fig. 1(a). From this figure, we can see that the chain mixes, i.e. moves with in the support of the PPDF, rapidly. A distinct feature of the MCMC estimation is the ease of extracting marginal distributions for the components of interest. In this paper, we use the kernel density estimation [30] to approximate the density of a sample $\{\rho_j\}_{j=1}^m$

$$p(\rho) = \frac{1}{m} \sum_{j=1}^m K(\rho|\rho_j). \tag{5.5}$$

Here we use $K(\rho|\rho_j) = N(\rho_j, \sigma_k^2)$ with $\sigma_k = 0.5$. The posterior density $p(\rho_6|Y)$ is shown in Fig. 1(b), and the posterior condition mean is 0.4914, which represents an excellent approximation of the exact value 0.5.

The numerical results for Example 1 with 1 and 5% noise in the data are shown in Fig. 2. In the figure, the vertical bar denotes the 95% credible interval, which quantifies the uncertainty of the mean. From this figure, we can see that the posterior conditional mean $\hat{\rho}$ is in excellent agreement with the exact solution and the credible interval shrinks as the noise level ϵ decreases. Furthermore, the results presented in Fig. 2 show clearly that our method also produces comparable accuracy as Ref. [8]. Hence the Bayesian inference approach provides stable numerical solutions to the inverse Robin problem associated with parabolic problem.

The numerical results for Example 1 with various levels of noise added into the data are presented in Table 1. In the table, the notation $\hat{\lambda}$ denotes the conditional mean of the regularization parameter λ . The hierarchical model (3.10) is flexible in handling the hyper-parameter λ . To show this, we consider Example 1 with 3% noise in the data. The prior density and the corresponding posterior density of the parameter λ are shown in Fig. 3. From this figure, the conditioning on the data greatly refines the distribution of the regularization parameter λ compared with its prior. Numerical results indicate that the automatically determined λ is rather optimal.

The numerical approximations of the boundary temperature $u(0, t)$ and $u(1, t)$, heat fluxes $q(0, t)$ and $q(1, t)$ are shown in Figs. 4 and 5, respectively. From these figures, we can see that with up to 5% noise in the data, the numerical

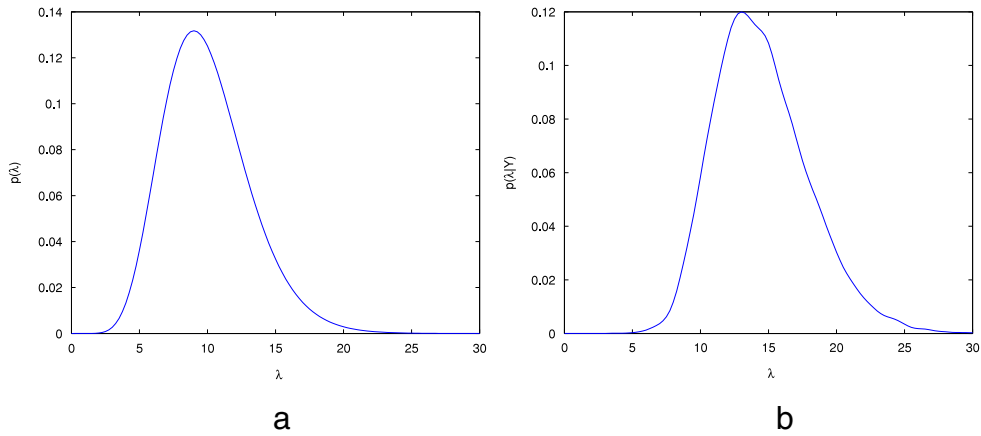


Fig. 3. (a) The prior density and (b) the posterior density of the scaling parameter λ for Example 1 with 3% noise added into the data.

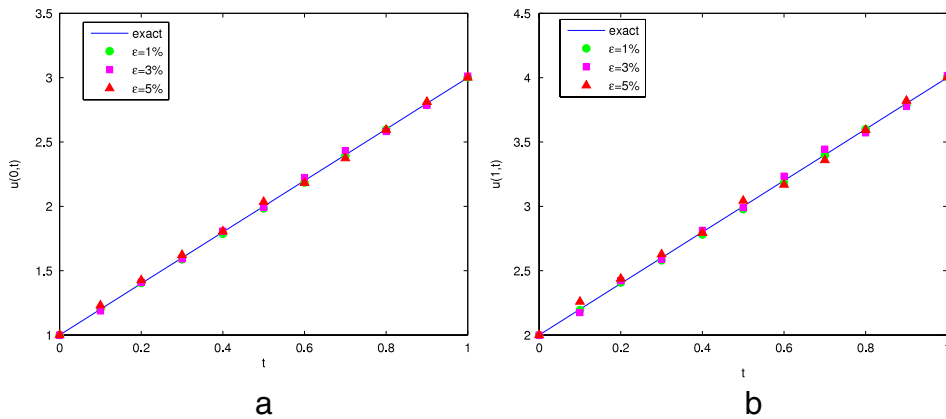


Fig. 4. The analytical and noisy boundary temperatures (a) $u(0, t)$ and (b) $u(1, t)$ for Example 1, with various amounts of noise added into the data.

Table 1
Numerical results for Example 1.

ϵ (%)	σ	$\hat{\lambda}$	rel (ρ)
1	0.04	12.07	0.0384
3	0.12	14.19	0.0807
5	0.20	15.05	0.0843

approximations are still in excellent agreement with the analytical solution. It should be mentioned that these numerical results are more accurate than the one reported in [10], where the approximation deviate from the exact solution when the noise is larger than 1%.

5.2. Nonsmooth solution

In this subsection, we consider two more challenging case of reconstructing a nonsmooth solution.

Example 2. The Robin coefficient $\rho(t)$ is a nonsmooth but continuous function

$$\rho(t) = \begin{cases} 2t, & 0 \leq t \leq 0.5, \\ 2 - 2t, & 0.5 < t \leq 1. \end{cases} \tag{5.6}$$

Example 3. The Robin coefficient $\rho(t)$ is a discontinuous function

$$\rho(t) = \begin{cases} 1, & 0.25 < t < 0.75, \\ 0, & \text{otherwise.} \end{cases} \tag{5.7}$$

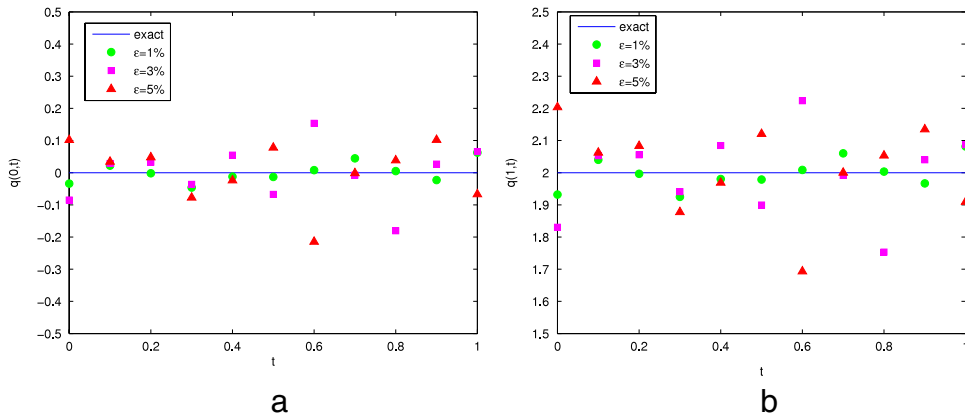


Fig. 5. The analytical and numerical heat fluxes (a) $q(0, t)$ and (b) $q(1, t)$ for Example 1 with various amounts of noise added into the data.

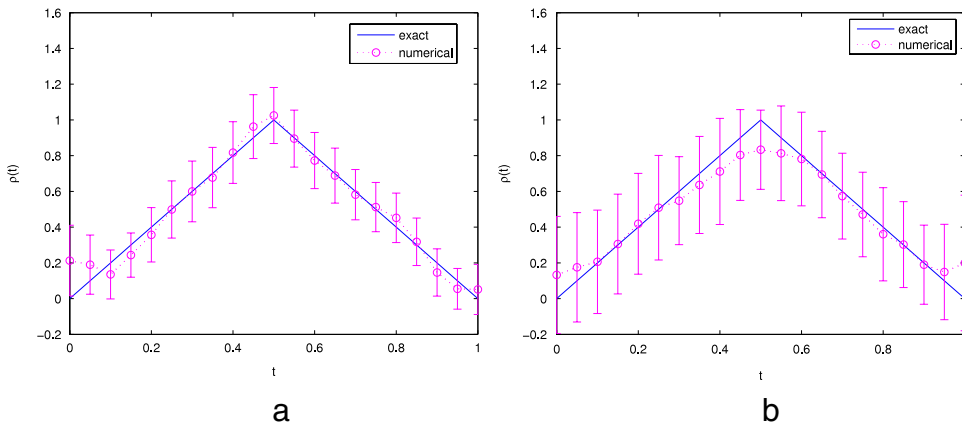


Fig. 6. The numerical results for Example 2 with (a) 1% and (b) 5% noise added into the data.

Table 2
Numerical results for Example 2.

ϵ (%)	σ	$\hat{\lambda}$	rel (ρ)
1	0.0537	20.85	0.0787
3	0.1611	21.08	0.1048
5	0.2686	21.77	0.1491

It should be mentioned that in Examples 2 and 3, the direct problem does not have an analytical solution. Thus the boundary temperature Y is obtained by solving the direct problem on a finer mesh in order to avoid the notorious ‘inverse crime’ [31].

The numerical results for Example 2 with 1% and 5% noise in the data are shown in Fig. 6. The posterior conditional mean $\hat{\rho}$ agrees reasonably well with the exact solution, and the credible interval shrinks as the noise level ϵ decreases from 5% to 1% albeit more slowly. Note that the probability bound is also adversely affected and not so sharp as for smooth solutions. The posterior densities of the hyper-parameter λ for Example 2 with 3% noise added into the data is shown in Fig. 7, whereas the posterior conditional means are presented in Table 2. The numerical results indicate that the posterior conditional mean $\hat{\lambda}$ is rather optimal.

Careful design of the proposal distribution $q(\rho|\rho^*)$ significantly affects the quality of the samples from the chain [32]. To illustrate this point, we plot $\gamma(s)$, the empirical autocovariance at lag s , in Fig. 8 for several random walk samples, varying the scale parameter of the proposal distribution σ_ρ . If σ_ρ is too large, e.g. $\sigma_\rho = 1$, the moves are large, but most proposals are rejected and the chain does not move often. If σ_ρ is too small, e.g. $\sigma_\rho = 0.001$, most proposed moves will be accepted but the chain will move slowly through the posterior support. Both of these situations are reflected in long correlations and poor mixing. With $\sigma_\rho = 0.04$, however, it exhibits short correlation length and good mixing.

Accurate reconstruction of discontinuous Robin coefficient is numerically very challenging. To illustrate this point we consider Example 3. The numerical results for Example 3 with 1% and 5% noise added into the data are presented in Fig. 9. From this figure, we can see that the numerical results are less accurate than those of Examples 1 and 2. It is not difficult to

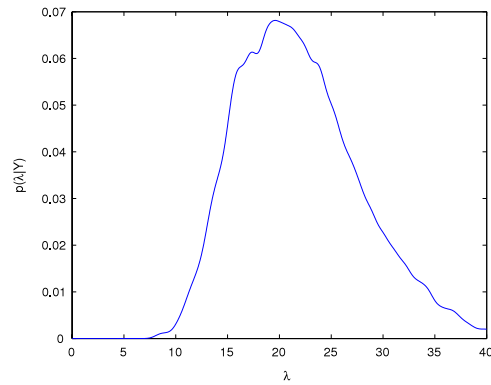


Fig. 7. The posterior density of the scaling parameter λ for Example 2 with 3% noise added into the data.

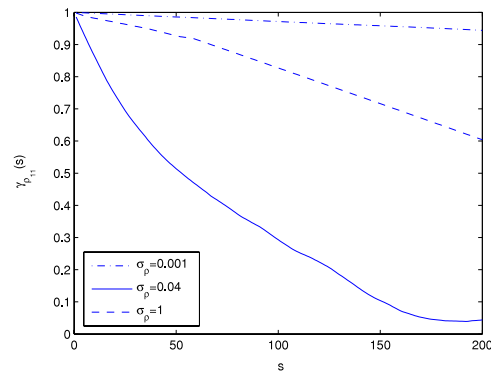


Fig. 8. The autocorrelation of ρ_{11} for Example 2 with 3% noise added into the data.

Table 3
Numerical results for Example 3.

ϵ (%)	σ	$\hat{\lambda}$	rel (ρ)
1	0.0568	34.03	0.1925
3	0.1136	36.89	0.2102
5	0.2840	31.99	0.3107

see that the recovered solution near the discontinuity points is not accurate. The total-variation prior [19] may be employed to circumvent the undesirable smoothing effect. Taking into consideration the ill-posedness of the problems, the results presented here are quite satisfactory. The posterior density of the regularization parameter λ for Example 3 with 3% noise added into the data is shown in Fig. 10. The posterior conditional mean $\hat{\lambda}$ of λ in this case is 36.89, see Table 3. Numerical results indicate that the automatically determined regularization parameter λ is rather optimal.

The foregoing numerical verifications indicate that the proposed method, i.e. the Bayesian inference approach, is efficient and accurate for reconstructing smooth Robin coefficients and also yields acceptable results for nonsmooth coefficients.

6. Conclusions

In this paper, a Bayesian statistical inference method is presented to identify a Robin coefficient in parabolic problems. The posterior distribution of an unknown Robin coefficient is computed from boundary temperature measurement by modeling the measurement errors as i.i.d. Gauss random variables. The MCMC algorithm was used to explore the posterior state space, and a MRF model was used to regularize the ill-posed inverse problem. The numerical results indicate that the Bayesian inference approach can yield an accurate solution with its uncertainty quantified and the hierarchical Bayesian formulation is capable of automatically determining an appropriate regularization parameter.

There are several potential extensions of the present method. Firstly, the extension of this approach to the two-dimensional case is straightforward, though more expensive. In particular, the required discretization of the domain implies a higher computational effort. Secondly, the proposed scheme can provide good estimates of the noise level [25,26]. However, these are deferred to future work.

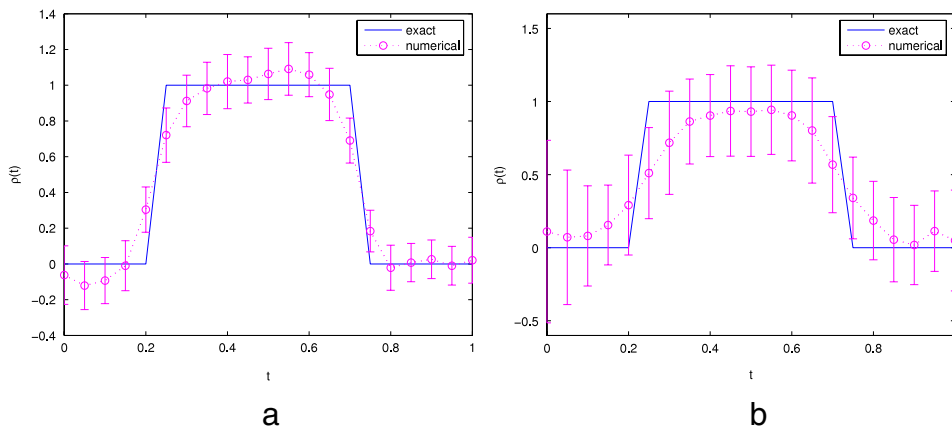


Fig. 9. The numerical results for Example 3 with (a) 1% and (b) 5% noise added into the data.

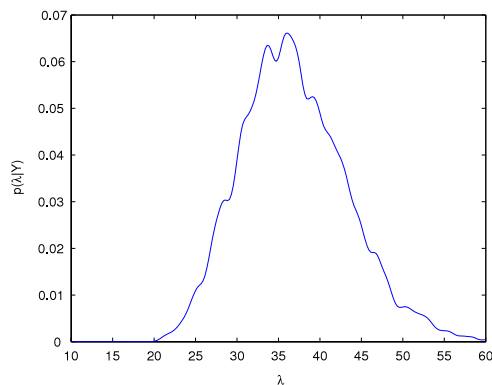


Fig. 10. The posterior density of the scaling parameter λ for Example 3 with 3% noise added into the data.

Acknowledgements

The authors would like to thank Dr. Bangti Jin for his valuable discussions and the referees for their constructive comments.

References

- [1] J. Hadamard, Lectures on the Cauchy Problem in Linear Partial Differential Equations, Oxford University Press, London, 1923.
- [2] O.M. Alifanov, Inverse Heat Transfer Problems, Springer, Berlin, 1994.
- [3] J. Beck, B. Blackwell, C.R. St-Clair Jr., Inverse Heat Conduction: Ill-posed Problems, Wiley, New York, 1985.
- [4] A.B. Kostin, A.I. Prilepko, Some problems of restoring the boundary condition for a parabolic equation, II, Differential Equations 32 (1996) 1515–1525.
- [5] M. Slodička, R. Van Keer, Recovery of the convective transfer coefficient in parabolic problems from a nonstandard boundary condition, in: N.E. Mastorakis (Ed.), Recent Advances in Applied and Theoretical Mathematics, 2000, pp. 209–213.
- [6] M. Slodička, R. Van Keer, Determination of a Robin coefficient in semilinear parabolic problems by means of boundary measurements, Inverse Problems 18 (2002) 139–152.
- [7] P.L. Masson, T. Loulou, E. Artioukhine, Estimation of a 2D convection heat transfer coefficient during a test: Comparison between two methods and experimental validation, Inverse Problems Sci. Eng. 12 (2004) 595–617.
- [8] F.L. Yang, L. Yan, T. Wei, The identification of a Robin coefficient by a conjugate gradient method, Internat. J. Numer. Methods Engrg. 78 (2009) 800–816.
- [9] X. Ling, R.G. Keanini, H.P. Cherukuri, A non-iterative finite element method for inverse heat conduction problems, Internat. J. Numer. Methods Engrg. 56 (2003) 1315–1334.
- [10] T.T.M. Onyango, D.B. Ingham, D. Lesnic, Reconstruction of heat transfer coefficients using the boundary element method, Comput. Math. Appl. 56 (2008) 114–126.
- [11] T.T.M. Onyango, D.B. Ingham, D. Lesnic, M. Slodička, Determination of a time-dependent heat transfer coefficient from non-standard boundary measurements, Math. Comput. Simul. 79 (2009) 1577–1584.
- [12] H.T. Chen, X.Y. Wu, Investigation of heat transfer coefficient in two-dimensional transient inverse heat conduction problems using the hybrid inverse scheme, Internat. J. Numer. Methods Engrg. 73 (2008) 107–122.
- [13] A.M. Osman, J.V. Beck, Investigation of transient heat transfer coefficients in quenching experiments, Trans. ASME, J. Heat Transfer 112 (1990) 843–848.
- [14] S. Chantasiriwan, Inverse heat conduction problem of determining time-dependent heat transfer coefficient, Int. J. Heat Mass Transfer 42 (2000) 4275–4285.
- [15] N.Z. Sun, W.G. Yeh, A stochastic inverse solution for transient groundwater flow: Parameter identification and reliability analysis, Water Resour. Res. 28 (1992) 3269–3280.
- [16] T.D. Fadale, A.V. Nenarokomov, A.F. Emery, Uncertainties in parameter estimation: The inverse problem, Int. J. Heat Mass Transfer 38 (1995) 511–518.
- [17] V.A.B. Narayanan, N. Zabarbas, Stochastic inverse heat conduction using a spectral approach, Internat. J. Numer. Methods Engrg. 60 (2004) 1569–1593.

- [18] B. Jin, J. Zou, Inversion of Robin coefficient by a spectral stochastic finite element approach, *J. Comput. Phys.* 227 (2008) 3282–3306.
- [19] J. Kaipio, E. Somersalo, *Statistical and Computational Inverse Problems*, Springer, New York, 2005.
- [20] C. Andrieu, N.D.E. Freitas, A. Doucet, M.I. Gordan, An introduction to MCMC for machine learning, *Mach. Learn.* 50 (2003) 5–43.
- [21] S. Geman, D. Geman, Stochastic relaxation, Gibbs distributions, and Bayesian restoration of images, *IEEE Trans. Pattern Anal. Mach. Intell.* 6 (1984) 721–741.
- [22] A. Malinverno, V.A. Briggs, Expanded uncertainty quantification in inverse problems: Hierarchical Bayes and empirical Bayes, *Geophysics* 69 (2004) 1005–1016.
- [23] J. Wang, N. Zabaras, A Bayesian inference approach to the inverse heat conduction problem, *Int. J. Heat Mass Transfer* 47 (2004) 3927–3941.
- [24] J. Wang, N. Zabaras, Hierarchical Bayesian models for inverse problems in heat conduction, *Inverse Problems* 21 (2005) 183–206.
- [25] B. Jin, J. Zou, A Bayesian inference approach to the ill-posed Cauchy problem of steady-state heat conduction, *Internat. J. Numer. Methods Engrg.* 76 (2008) 521–544.
- [26] B. Jin, Fast Bayesian approach for parameter estimation, *Internat. J. Numer. Methods Engrg.* 76 (2008) 521–544.
- [27] S. Parthasarathy, C. Balaji, Estimation of parameters in multi-mode heat transfer problems using Bayesian inference-Effect of noise and a priori, *Int. J. Heat Mass Transfer* 51 (2008) 2313–2334.
- [28] Z.Z. Sun, *Numerical Solution for Partial Differential Equations*, Science Press, Beijing, 2005.
- [29] A. Gelman, J.B. Carlin, H.S. Stern, D.B. Rubin, *Bayesian Data Analysis*, 2nd ed., CRC Press, Boca Raton, FL, 2004.
- [30] J.E. Gentle, *Elements of Computational Statistical*, Springer, New York, 2002.
- [31] J. Kaipio, E. Somersalo, *Statistical inverse problems: Discretization, model reduction and inverse crimes*, *J. Comput. Appl. Math.* 198 (2007) 193–504.
- [32] J.S. Liu, *Monte Carlo Strategies in Scientific Computing*, Springer, New York, 2001.